Excerpt from the Proceedings of the 2011 COMSOL Conference in Boston

Hybrid FEM-BEM approach for two- and three-dimensional open boundary magnetostatic problems

A. Weddemann*, D. Kappe**, A. Hütten**

* Research Laboratory of Electronics, Massachusetts Intstitute of Technology, 77 Massachusetts Ave, MA 02139, USA, weddeman@mit.edu
** Thin Films and the Physics of Nanostructures, Bielefeld University, Bielefeld, Germany

ABSTRACT

In order to eliminate additional degrees of freedom in the surrounding domain of a charged or polarized object, we implement an open boundary method based on a hybrid FEM-BEM approach which is tested for magnetostatic problems. The underlying functional dependency of domain and boundary variables entails a sparsity decrease of the system matrix with an increasing surface area to volume ratio. Such a case is commonly at hand if systems with a high aspect ratio are considered. Therefore, we also propose an effective way which allows for the treatment of such systems in a simplified two-dimensional form without neglecting the three-dimensional characteristics of the external field. The approach is tested for the cases of a three-dimensional homogeneously magnetized sphere and a thin magnetic sheet.

Keywords: magnetostatics, open boundary models, boundary element method

1 INTRODUCTION

Recent trends in fore-front technological methods venture into a progressive miniaturization of functional devices down to the micro- or even nanoscale [1], [2]. Commonly, these systems combine continuum mechanical and electromagnetic aspects and are widely summarized within the field of MEMS- or NEMS-technology (**M**icro-/**N**ano-**E**lectro-**M**echanical-**S**ystems). With strongly reduced dimensions, different effects become predominant in comparison to the macroscale. In particular, strong variations of physical properties may occur on even short length and time scales. Therefore, an accurate evaluation of all contributions involved proves crucial for the design of novel devices. In this regard, finite element methods provide a strong tool for the numerical analysis of such systems. In comparison to, e.g., finite difference techniques, the spatial discretization of the physical domain into triangular/tetrahedral subdomains allows for a precise approximation of the model geometry.

However, one particular inherent characteristic about Maxwell's equations introduces complications when dealing with the electromagnetic properties. While most mechanical quantities are local, i.e., their values at a specific space point can be obtained by the evaluation of various material properties at the respective position, magnetic fields exhibit a non-local nature. As an example, we consider a magnetic block as shown in Figure 1(a) that is homogeneously magnetized with the magnetization parallel to the negative x-axis. Of course, we would expect its deformation under some sort of mechanical stress to be independent from the topology of the surrounding space, only forces along the volume or the surface are of importance. Similarly, in order to estimate magnetic forces on the block, we are only interested in the magnetic field along the volume of the block itself. Unfortunately, the magnetic field at a given point does not only depend on properties at this particular point but the entire (unbounded) space needs to be taken into account.

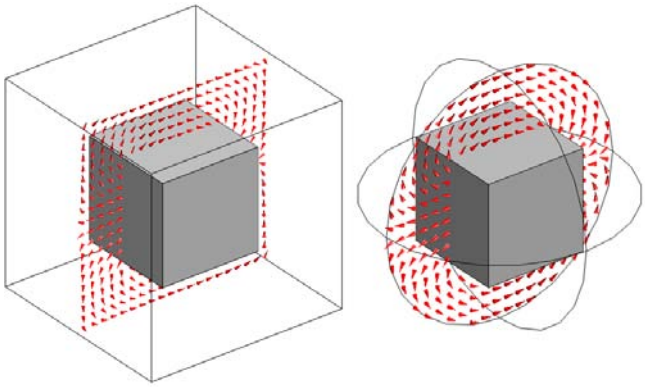

Figure 1: Influence of the choice of the domain cut-off for (a) rectangular and (b) spherical exterior domain. Depending on the choice of the exterior, strong deviations from the exact solution may be present on the magnetic object (gray block).

Since finite element techniques can only deal with finite domains, an auxillary domain such as shown in Figure 1 needs to be introduced. These non-physical boundaries result in an additional error in the numerical solution which increases with a decreasing domain size. As a rule of thumb, the employment a cut-off region with a radius of about five times the size of the geometrical size scale leads to results which are only slighly affected by the assumption of a finite domain. In the

past, different techniques for a more efficient treatment of the outer domains have been proposed. An example is the introduction of *infinite elements* which map a certain part of the geometry to infinity. Even though such techniques decrease the numerical error, they still require to solve the equations on an extended geometry where the solution is not of interest and, therefore, entail an increased number of degrees of freedom and a higher calculation time. In this work, we implement a method to eleminate all degrees of freedom which are irrelevant for the physical model.

2 GOVERNING EQUATIONS

We restrict our analysis to the case of magnetostatics. The approach presented and all resulting equations are not restricted to micro- or nano-dimensional systems but valid on *all* length scales. For our systems, we assume that all external current densities vanish, $\mathbf{j}_{\text{ext}} \equiv \mathbf{0}$. Therefore, Maxwell's equations of magnetostatics are given by

$$\nabla \cdot \mathbf{B} = 0 \tag{1}$$

$$\nabla \times \mathbf{H} = \mathbf{0} \tag{2}$$

where $\mathbf{H}$ denotes the magnetic field, and $\mathbf{B}$ the magnetic flux density. With the curl of $\mathbf{H}$ zero in the entire space, $\mathbf{H}$ may be written as the gradient of a scalar potential φ, in the form $\mathbf{H} = -\nabla\varphi$. Further, magnetic field and flux density are connected by

$$\mathbf{B} = \mu_0(\mathbf{M} + \mathbf{H}) \tag{3}$$

with $\mathbf{M}$ the magnetization of an object which is $\mathbf{0}$ in the case of vacuum.

2.1 Scalar equations

By substitution of equation (3) into equation (1) and employing the potential representation of $\mathbf{H}$, we obtain the governing equation for the magnetic potential φ which is given by the Poisson equation

$$\Delta\varphi = \nabla \cdot \mathbf{M} \tag{4}$$

with Δ the Laplacian operator. If we consider magnetic objects surrounded by a non-magnetic medium (or also another magnetic object with different magnetic properties), the solution needs to satisfy certain boundary conditions. Similar to electrostatic problems where the electric potential in the direction of the surface normal $\hat{\mathbf{n}}$ exhibits a jump given by the electric surface charge σ along the interface, the jump in the magnetic potential is given by the outward components of the magnetization vector $\mathbf{M}$

$$\frac{\partial\varphi}{\partial\hat{\mathbf{n}}} = \hat{\mathbf{n}} \cdot \mathbf{M}. \tag{5}$$

In principal, we need to find a solution of equation (4) for all space points $\mathbf{r} \in \mathbb{R}^n$ which satisfies boundary conditions of type (5) along all material interfaces.

2.2 Integral formulation

In order to eliminate the degrees of freedom (DOF) along the unbounded domain where $\mathbf{M} \equiv \mathbf{0}$, we introduce the decomposition $\varphi = \varphi_1 + \varphi_2$. Let V_{mag} denote the magnetic volume with boundary Γ, we assume φ_1 to be a solution of

$$\begin{array}{rcll} \Delta\varphi_1 & = & \nabla \cdot \mathbf{M} & \forall \mathbf{r} \in V_{\text{mag}} \\ \varphi_1 & = & 0 & \forall \mathbf{r} \in \mathbb{R}^n \backslash V_{\text{mag}} \\ \frac{\partial}{\partial\hat{\mathbf{n}}}\varphi_1 & = & \hat{\mathbf{n}} \cdot \mathbf{M} & \forall \mathbf{r} \in \Gamma \end{array} \tag{6}$$

where $\frac{\partial}{\partial\hat{\mathbf{n}}}$ denotes the derivative in the direction of the surface normal $\hat{\mathbf{n}}$. With this particular choice of φ_1, φ_2 is a solution of the homogeneous Laplace equation and, consequently, a harmonic function. The theory of harmonic functions provides an integral formulation which allows for the evaluation of φ_2 at any given point $\mathbf{r} \in \mathbb{R}^n$

$$\varphi_2(\mathbf{r}) = \int_\Gamma \varphi_1(\mathbf{r}') \, \frac{\partial}{\partial\hat{\mathbf{n}}} G(\mathbf{r}, \mathbf{r}') \, \mathrm{d}\mathbf{r}'. \tag{7}$$

The function $G(\mathbf{r}, \mathbf{r}')$ denotes the *Greens function* of the boundary value problem which depends on the system dimension n with respective representations

$$G(\mathbf{r}, \mathbf{r}') = \frac{1}{2\pi} \ln(|\mathbf{r} - \mathbf{r}'|) \qquad \text{for } n = 2$$

$$G(\mathbf{r}, \mathbf{r}') = \frac{1}{4\pi} \frac{1}{|\mathbf{r} - \mathbf{r}'|} \qquad \text{for } n = 3$$

However, the evaluation of the integral expression is numerically costly (storage of $\mathcal{O}(N^{5/3})$, with N the number of elements [3]). Therefore, instead of calculating expression (7) on the entire domain V_{mag}, we restrict the evaluation to the domain boundary Γ and treat these values as the data of the corresponding Dirichlet problem. Therefore, for a three-dimensional system, φ_2 needs to be a solution of

$$\begin{array}{rcll} \Delta\varphi_2 & = & 0 & \forall \mathbf{r} \in V_{\text{mag}} \\ \varphi_2(\mathbf{r}) & = & \int_\Gamma \varphi_1(\mathbf{r}') \, \frac{\partial}{\partial\hat{\mathbf{n}}} G(\mathbf{r}, \mathbf{r}') \, \mathrm{d}\mathbf{r}' & \\ & & + \left(\frac{\Omega(\mathbf{r})}{4\pi} - 1 \right) \varphi_1(\mathbf{r}) & \forall \mathbf{r} \in \Gamma \end{array} \tag{8}$$

with $\Omega(\mathbf{r})$ the solid angle of the surface element at the respective position $\mathbf{r}$. The additional term results from taking the limit $\mathbf{r} \to \Gamma$ due to the singularities in the Greens functions. For all smooth boundaries Ω is given by 2π, an example for a non-smooth surface will be discussed in section 3.2

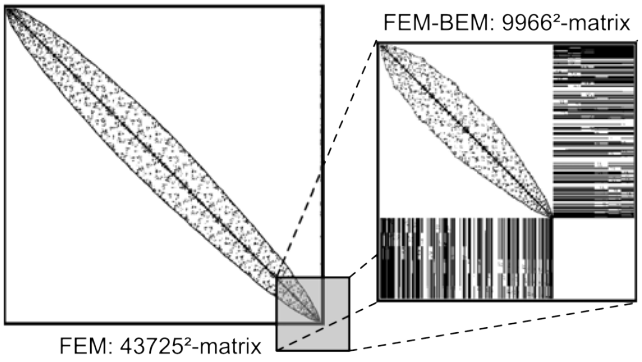

Figure 2: Sparsity plots for system matrices assembled in an FEM- (left) and a hybrid FEM-BEM framework (right). Even though the FEM-BEM matrix is of much smaller dimension (gray area), it may contain a similar number of non-zero matrix elements.

mesh type	Elements	Bound. Ele.	#DOFs
FEM	31944	1596	43725
FEM/BEM	2128	528	6798

Table 1: Different mesh parameters for the cube system discretized in an FEM- and FEM-BEM framework.

2.3 Hybrid FEM-BEM method

At this point, we have successfully eliminated the auxiliary domain, the governing equations (6) and (8) are completely specified by the physical properties of the domain V_{mag}. Since we have effectively recast properties of the domain to the domain boundary while some parts remain governed by subdomain equations, this method is often refered to as *hybrid FEM-BEM method*. Obviously, such an approach results in a significant reduction of the number of DOFs of the system. In order to give an example on how this formulation affects the numeric parameters, we consider the magnetic cube shown in Figure 1 with a side length of $a = 1$. If a high accuracy is desired, the surrounding sphere for the pure FEM approach should have approximately a radius of five times the size scale of the considered geometrical structure. Therefore, we set $R = 5$. The mesh parameters are chosen with a maximum mesh size of 0.2 on the cube with a growth rate of 1.2 on the surrounding sphere. The corresponding mesh for the hybrid method is given by the partial mesh of the sole cube. Mesh parameters and resulting number of DOFs are given in Table 1.

Even though we need to solve for two variables φ_1, φ_2 by emploment of the hybrid approach, the reformulation of the original equations and the entailed elimination of the surrounding domain results in a reduction of the number of DOFs down by more than 80%. On top of that, it is important to note that the combined equations (6) and (8) are still exact and do not introduce an additional approximation error due to an arbitrary cut-off parameter. However, as a general law of nature states the conservation of the complexity of a problem, it is universally known that whenever things look to good too be true, they usually aren't. So, what makes the application of this method challenging or in other words what are the cost for the reduced number of DOFs?

In order to understand the numerical issues which result from the reformulation of the original problem, some basic knowledge about finite element methods in general is required: In a first step, when solving a numerical model, the stiffness matrix of the system is assembled. This matrix is a quadratic $N \times N$-matrix with N the number of DOFs. An advantage of these system matrices is their sparsity. A matrix component A_{ij} is only non-zero, when its indices correspond to overlapping basis functions or, in other words, when individual nodes of the finite element mesh are coupled/contiguous to each other. A typical system matrix is shown in Figure 2(a), only the black dots correspond to entries with a value unequal to zero. For sparse matrices, very efficient algorithms for numerical operations such as LU-decomposition are known which result in a decreased solving time for the linearized set of equations.

Now, what happens when expressions such as equation 7 are introduced? Basically, all elements are coupled to the boundary elements and, therefore, we lose the degree of sparsity as is shown in Figure 2(b). Even though the number of DOFs may go down, we might still end up with a system that may no longer be solvable with spezialized solvers such as UMFPACK because these solvers may not perform well on dense matrices.

3 THREE-DIMENSIONAL MODELS

In order to test advantages and limitations of this approach implemented into COMSOL Multiphysics, we will employ the FEM-BEM frame for the solution of various geometries. The application of this method to full three-dimensional problems is straight forward. The settings chosen in the following sections cover all main aspects necessary for the analysis of an arbitrary three-dimensional magnetostatic problem.

3.1 Smooth surfaces: the sphere

As a benchmark model, we choose the homogeneously magnetized sphere of radius $R = 1$ and magnetization $\mathbf{M} = \hat{\mathbf{z}}$. The centre of the sphere is set as the origin of the coordinate system. By employment of the axial symmetry of the geometry, the magnetic scalar potential φ can be expanded into a series of Legendre polynoms

#Elements	#Bnd. Elements	$\Delta H^1(\varphi_h)$	t_{sol} [s]
97	80	0.0757	1.466
324	152	0.0470	1.981
1251	320	0.0324	3.113
9098	1240	0.0230	17.191
18119	3495	0.0036	34.725

Table 2: H^1-error and calculation time for different mesh settings.

which results in the analytic solution [4]

$$\mathbf{H}(\mathbf{r}) = -\frac{1}{3}\mathbf{M} \qquad r < R \qquad (9)$$

$$\mathbf{H}(\mathbf{r}) = \frac{1}{4\pi}\left(\frac{3(\mathbf{M}\cdot\mathbf{r})\mathbf{r}}{|\mathbf{r}|^5} - \frac{\mathbf{M}}{|\mathbf{r}|^3}\right) \qquad r > R \qquad (10)$$

As a quality measure, we evaluate the H^1-error of the approximate solution $\varphi_h = \varphi_{h,1} + \varphi_{h,2}$ in comparison to the exact solution φ

$$\begin{aligned}\Delta H^1(\varphi_h) &= |\varphi_h - \varphi|_{H^1(V_{\text{mag}})} \\ &= \left(\int_{V_{\text{mag}}} |\nabla\varphi_h(\mathbf{r}) - \nabla\varphi(\mathbf{r})|^2 \,\mathrm{d}\mathbf{r}\right)^{-1/2}\end{aligned}$$

In equation (8), we may set the solid angle $\Omega \equiv 2\pi$ since the surface of the sphere is smooth. The resulting errors and solution times for different mesh cases are given in table 2.

It needs to be pointed out that a high amount of the calculation time is necessary for the assembly of stiffness and constraint matrices and full FEM schemes may, therefore, reach higher perfomances. For the sphere example, an error of $\Delta H^1 = 7.9 \times 10^{-3}$ was achieved with a calculation time of 3.2s on a finite element grid with more than 40,000 DOFs. However, at this point, we may notice that the FEM-BEM solution for the magnetic field converges to the exact solution in regard to the function space $L^2(V_{\text{mag}})$ with increasing mesh resolution.

3.2 Angular surfaces: the cube

In contrast to the preliminary section, geometries with edges such as the cube do not satisfy the condition $\Omega \equiv 2\pi$ along all points of the boundary and an inappropriate choice results in deviations from the actual solution. As a test case, we consider a cubic geometry with side length $a = 1$ and magnetization $\mathbf{M} = \hat{\mathbf{z}}$. As shown in Figure 3(a), a constant solid angle results in non-physical deviations along the geometry edges.

However, the correct Ω-values along the edges can easily be deduced: a smooth surface may be locally approximated by a half space which corresponds to half the full solid angle of 4π. Along the edges, the local approximation resembles half and in corners a quarter of a half space so that the respective values are given by π and $\pi/2$. For a more rigorous and general discussion about solid angles refer to, e.g., [5].

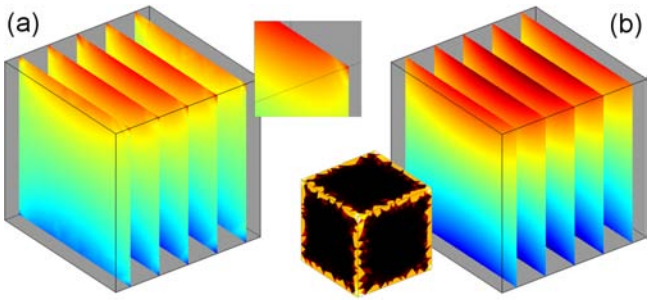

Figure 3: FEM-BEM solutions for φ under the assumption $\mathbf{M} = \hat{\mathbf{z}}$ for a cubic geometry with side length $a = 1$. The colorscale ranges linearly from -0.207 (blue) to 0.207 (red). (a) shows the results of a calculation carried out with a constant value for the solid angle $\Omega \equiv 2\pi$. As highlighted in the inset, strong (unphysical) features are present along the edges. (b) presents the result with the corrected values Ω, the inset shows the L^2-approximation of the solid angle which is 2π, π and $\pi/2$ along the surfaces (dark), edges (orange) and in the corners (bright), respectively.

Unfortunately, this assignment does not make sense for L^2-functions on neither the domain V_{mag} nor the boundary Γ since edges and corners each form null sets in the respective case. For our approach, it is sufficient to have a proper definition along the boundary since Ω is part of the Dirichlet data only. Therefore, we need an extension $\Omega \in L^2(\Gamma)$ which was realized by an additional weak boundary equation. The result is shown in the inset of Figure 3(b). Dark areas correspond to a value of 2π, orange to a value of π while the angle at the corners is set to $\pi/2$ (bright).

The application of this approximation of the solid angle reduces edge deviations as shown in Figure 3(b). The magnetic potential ranges between -0.207 and 0.207 which coincides with the results obtained by pure FEM methods.

3.3 Inclusion of an outer domain

Even though we have gone through quiet some efforts to eliminate all exterior DOFs, there may be systems, where the magnetic field outside the magnetic volume is of interest. A common example is formed by magnetic particles that interact with a MEMS/NEMS-device but are small enough that their perturbation of the field configuration may be omitted [6].

Again, it is preferable to model as little additional

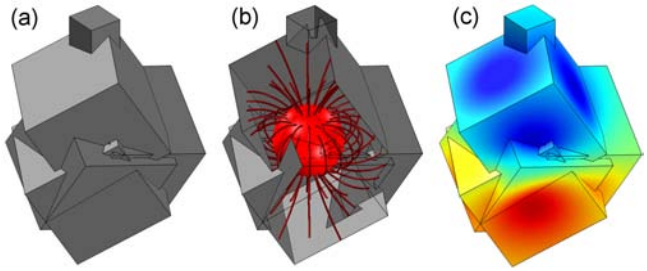

Figure 4: FEM-BEM solution for the magnetic field outside a homogeneously magnetized sphere for an arbitrarily shaped physical domain with neutral boundaries. (a) shows the arbitrary domain, (b) the magnetic stray field inside. Subplot (c) shows the distribution of the magnetic potential along the surface employed for the Dirichlet problem of φ_2.

volume as possible without introduction of unphysical boundary effects. Figure 4 shows an example of an arbitrarily shaped exterior domain with a homogeneously magnetized sphere inside. In principal, the magnetic stray field of the sphere can be calculated by evaluating the inner magnetic potential in a first step and, afterwards, by employing equation (7) to obtain φ on the outer regions. Since numerical integrations are very time consuming, we restrict the integration to the domain boundaries again. The potential on the sphere is calculated as explained above, the outer region follows from the homogeneous Laplace equation $\Delta\varphi_2 = 0$ with the integral values acting as Dirichlet data on both, inner and outer boundaries. Note that the variable φ_1 does not add additional DOFs since it was set to $\varphi_1 \equiv 0$ along all non-magnetic domains.

The result of the calculation is shown in Figure 4. We find that the magnetic stray field is not influenced by the presence of (non-physical) boundaries and resembles a perfect dipolar characteristic.

4 A TWO-DIMENSIONAL APPROXIMATION

As explained in section 2.3, the system matrix of the hybrid FEM-BEM method becomes increasingly dense the more surface elements can be found in the model. In particular, geometries with a high aspect ratio or more generally with a high surface to volume ratio should not be modelled staight forward in a three-dimensional fashion. Since the magnetic stray field of a thin (two-dimensional) magnetic layer is three-dimensional, a reduction of the dimensionality is not possible in FEM frameworks. For the FEM-BEM method, we will develop an effective two-dimensional formulation under some reasonable physical assumptions.

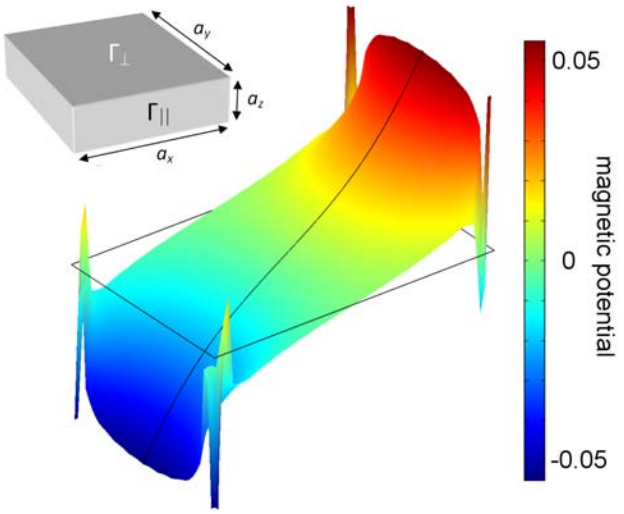

Figure 5: Magnetic properties of a homogeneously magnetized sheet of dimensions $a_x = 1.2$, $a_y = 0.8$ and $a_z = 0.1$, with $\mathbf{M} = \hat{\mathbf{x}}$. The inset shows a schematic representation, the surface plot the magnetic potential φ calculated in the FEM-BEM framework.

In order to model a thin magnetic layer, we may not employ the two-dimensional expression of the Greens function since this would correspond to a cuboid of infinite length in the out-of-plane direction. Such an approach would result in an overestimation of the resulting stray fields since a much higher amount magnetic material is contained. Instead, we consider the block shown Figure 5 with side lengths a_x, a_y and a_z, where we assume the block height to be much smaller than the lateral dimensions, $a_z \ll a_x, a_y$. According to Figure 5, the boundary integration may be split up into

$$\int_\Gamma \varphi_1 \frac{\partial G}{\partial \hat{\mathbf{n}}}\,\mathrm{d}\mathbf{r}' = \int_{\Gamma_{||}} \varphi_1 \frac{\partial G}{\partial \hat{\mathbf{n}}}\,\mathrm{d}\mathbf{r}' + \int_{\Gamma_\perp} \varphi_1 \frac{\partial G}{\partial \hat{\mathbf{n}}}\,\mathrm{d}\mathbf{r}' \qquad (11)$$

with $\Gamma_{||}$ and $\Gamma_\perp$ the respective surface elements with unit normals parallel and perpendicular to the xy-plane. If the lateral dimensions of the sheet are very low, the magnetic configuration is usually confined in the sheet plane itself [7] and, therefore, the average outward component $\langle m_z^2 \rangle$ is very small. Consequently, we have $\varphi_1(\mathbf{r}) \approx \varphi_1(x, y)$ and, therefore, it is possible to show

$$\begin{aligned}\int_{\Gamma_\perp} \varphi_1 \frac{\partial G}{\partial \hat{\mathbf{n}}}\,\mathrm{d}\mathbf{r}' &= \int \varphi_1 \left(\int \frac{\partial G}{\partial \hat{\mathbf{n}}}\,\mathrm{d}z' \right) \mathrm{d}x'\,\mathrm{d}y' \\ &= -\frac{a_z}{4\pi} \int_{\Gamma_\perp} \frac{\varphi_1\,\mathrm{d}x'\,\mathrm{d}y'}{\left(\Delta\mathbf{r}_{xy}^2 + a_z^2/4\right)^{3/2}}\end{aligned}$$

and

$$\int_{\Gamma_{||}} \varphi_1 \frac{\partial G}{\partial \hat{\mathbf{n}}}\,\mathrm{d}\mathbf{r}' = \frac{a_z}{4\pi} \int \varphi_1 \frac{\hat{\mathbf{n}} \cdot \Delta\mathbf{r}_{xy}}{|\Delta\mathbf{r}_{xy}|^3}\,\mathrm{d}\mathbf{r}'.$$

with $\Delta\mathbf{r}_{xy} = (x - x')\hat{\mathbf{x}} + (y - y')\hat{\mathbf{y}}$. A result for the calculation is shown in Figure 5. The subdomain shows the correct expected behavior, however, deviations can be found in the corners of the domain which are due to singularities of the integrand. Here, further tests will be necessary in the future to provide a smoother boundary behavior.

The calculation time of the hybrid approach (0.15 s) is significantly lower than the resulting values for the FEM framework (1.72 s). Additionally, the block height a_z enters the governing equations only as a numeric parameter in the integration along $\Gamma_\perp$ for the FEM-BEM framework, but leads to an increased number of elements (in order to maintain the minimal element quality) when applying an FEM scheme. Therefore, calculation times are independent of the value a_z in the first case while in the latter, they rapidly increase with decreasing film thickness. Therefore, this method might provide a valuable tool, especially, in the field of thin ferromagnetic film devices. For more information on this field of applications, see also *Ferromagnetic materials for MEMS- and NEMS-devices* in these conference proceedings [8].

CONCLUSION AND OUTLOOK

We have successfully implemented a hybrid FEM-BEM method into COMSOL Multiphysics and shown that this approach allows for an open boundary modeling of electromagnetic fields. At the current stage, the implementation does not provide significant performance advantages in respect to calculation time or memory requirements for full three-dimensional models due to the loss of sparsity of the stiffness matrix and the highly spezialized solvers applied. However, the additional employment of modern techniques such as the H^2-method form promising candidates a for further improvement and may result in a valuable tool for the efficient calculation of electromagnetic fields. In contrast to three-dimensional systems, the proposed method offers a strong performance increase for systems that can be reduced to a two-dimensional model.

Acknowledgements

A. Weddemann gratefully acknowledges the financial support of the Alexander von Humboldt foundation.

REFERENCES

[1] A. Weddemann, C. Albon, A. Auge, F. Wittbracht, P. Hedwig, D. Akemeier, K. Rott, D. Meiner, P. Jutzi, A. Hütten. *How to design magneto-based total analysis systems for biomedical applications.* Biosens. Bioelec. *26*, 1152-1163, **2010**.

[2] A. Weddemann, I. Ennen, A. Regtmeier, C. Albon, A. Wolff, K. Eckstädt, N. Mill, M. Peter, J. Mattay, C. Plattner, N. Sewald, A. Hütten. *Review and outlook: from single nanoparticles to self-assembled monolayer and granular GMR sensors.* Beilstein J. Nanotech. *1*, 75-93, **2010**.

[3] D.R. Fredkin, T.R. Koehler. *Hybrid method for computing demagnetization field.* IEEE Trans. Magn. *26*, 415-417, **1990**.

[4] J.D. Jackson. *Classical Electrodynamics*, 2nd ed., Wiley, New York **1975**.

[5] D.A. Lindholm. *Three-Dimensional Magnetostatic Fields from Point-Matched Integral Equations with Linearly Varying Scalar Sources.* IEEE Trans. Magn. *20*, 2025-2032, **1984**.

[6] N. Pamme. *Magnetism and Microfluidics.* Lab Chip *6*, 24-38, **2006**.

[7] A. Weddemann, A. Auge, C. Albon, F. Wittbracht, A. Hütten. *On the resolution limits of tunnel magnetoresistance sensors for particle detection* New J. Phys. *11*, 113027, **2009**.

[8] A. Weddemann, J. Jadidian, Y.S. Kim, S.R. Khushrushahi, M. Zahn. *Ferromagnetic materials for MEMS- and NEMS-devices.* Proc. COMSOL Conf., Boston, **2011**.